Molecular Motors in Aqueous Environment

Lubbe, Anouk S.; Böhmer, Christian; Tosi, Filippo; Szymanski, Wiktor; Feringa, Ben L.

Published in:
Journal of Organic Chemistry

DOI:
10.1021/acs.joc.8b01627

Publication date:
2018

JOC The Journal of Organic Chemistry

Article

Cite This: J. Org. Chem. 2018, 83, 11008−11018

pubs.acs.org/joc

Molecular Motors in Aqueous Environment

Anouk S. Lubbe,[†] Christian Böhmer,[†] Filippo Tosi,[†] Wiktor Szymanski,*[,†,‡] and Ben L. Feringa*[,†]

[†]Center for Systems Chemistry, Stratingh Institute for Chemistry, University of Groningen, Nijenborgh 4, 9747 AG Groningen, The Netherlands

[‡]Department of Radiology, University of Groningen, University Medical Center Groningen, Hanzeplein 1, 9713 GZ Groningen, The Netherlands

Supporting Information

ABSTRACT: Molecular motors are Nature's solution for (supra)molecular transport and muscle functioning and are involved in most forms of directional motion at the cellular level. Their synthetic counterparts have also found a myriad of applications, ranging from molecular machines and smart materials to catalysis and anion transport. Although light-driven rotary molecular motors are likely to be suitable for use in an artificial cell, as well as in bionanotechnology, thus far they are not readily applied under physiological conditions. This results mainly from their inherently aromatic core structure, which makes them insoluble in aqueous solution. Here, the study of the dynamic behavior of these motors in biologically relevant media is described. Two molecular motors were equipped with solubilizing substituents and studied in aqueous solutions. Additionally, the behavior of a previously reported molecular motor was studied in micelles, as a model system for the biologically relevant confined environment. Design principles were established for molecular motors in these media, and insights are given into pH-dependent behavior. The work presented herein may provide a basis for the application of the remarkable properties of molecular motors in more advanced biohybrid systems.

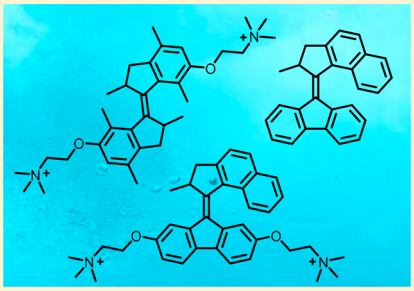

INTRODUCTION

The use of molecular photoswitches has enabled the noninvasive control of biological systems and functions by light.[1] Various classes of photochromic molecules, including azobenzenes,[2] diarylethenes,[3] spiropyrans,[4] and fulgides,[5] have been used in applications including regulation of peptide[6] and lipid[7] structure, enzyme inhibition,[8] and photocontrol of DNA structure and function.[9] Incorporation of molecular photoswitches into the structure of bioactive small molecules, along the principles of photopharmacology,[10] has further expanded those possibilities toward the regulation of antibiotic activity,[11] neuronal signaling,[12] receptor activation,[13] tubulin polymerization inhibition,[14] histone deacetylase,[15] and kinase activity[16] and the functioning of pancreatic beta cells,[17] among others.

A special type of photoresponsive molecules, light-driven rotary molecular motors based on overcrowded alkenes, were first reported in 1999[18] and have since been the subject of detailed investigation.[19] A thorough understanding of the exact mechanism of rotation has been acquired,[20−22] and the unique properties of molecular motors have found a myriad of applications. The inversion in helical chirality that accompanies each rotational step has been exploited to govern, among others, the outcome of asymmetric catalysis,[23] to induce unidirectional rotation of a microscopic glass rod,[24] and to modulate preference for the binding of chiral anions.[25] When used as molecular photoswitches, molecular motors are robust and highly efficient. The multiple switch states have been used to induce gel−solution transitions,[26] change the morphology of nanotubes,[27] and influence peptide secondary structure.[28] Surface functionalization[29−31] has opened the door to potential applications in information storage, in which the four-state switching cycle of molecular motors is of particular appeal, and may also be used for amplification to achieve collective behavior. Finally, the conversion of rotary into linear motion has been demonstrated by the directional movement of a motorized nanocar across a copper surface.[32]

However, despite the recent surge in interest in the application of photoswitches in biological systems and in pharmacology,[10−17] molecular motors are thus far left out of the arsenal that makes up the primary tools for photopharmacology and other biological applications. Directional motion is ubiquitous in motor proteins, such as ATPase, kinesin, and myosin. These dynamic systems have served as a source of inspiration for the development of artificial molecular motors. The application of synthetic rotary molecular motors in a biological setting may lead to a whole new level of control over biological function. Our group has reported one example of a molecular motor incorporated in a peptide, where photoswitching of the motor could induce structural changes.[28] However, the hybrid shows strong aggregation behavior, which was attributed to the hydrophobic core of the motor. This observation revealed the primary issue regarding the application of molecular motors in aqueous media, i.e., their insolubility in water. An outstanding challenge is the design of water-soluble, light-driven molecular motors.

Received: June 28, 2018
Published: August 22, 2018

All light-driven overcrowded alkene-based molecular motors, from the first to the third generation, share the same stilbene core structure.[18,20,33] which renders them inherently hydrophobic. A second-generation molecular motor, functionalized with alkyl and PEG chains, could be operated in water, but as this motor was designed to be an amphiphile, it formed large supramolecular aggregates.[27] Additionally, a surface-bound second-generation motor was used to modulate surface wettability, but this application was strongly dependent on hydrophobic effects.[31] Harada and co-workers have reported a first-generation molecular motor functionalized with short peptide sequences, which was studied using UV−vis spectroscopy in aqueous solution.[34] However, potential aggregation was not investigated. It is highly likely that these structure behave similar to the peptides reported by our group (vide supra) and experience aggregation.

The most straightforward approach to solving this problem and creating molecular motors fully soluble in water is to functionalize a molecular motor with polar, solubilizing groups. As an alternative approach, molecular motors could be operated in the membrane or other apolar environments in the cell. In recent publications, a molecular motor was used as a highly efficient photoswitchable anion receptor[35] or as a disruptive agent to destabilize the cell membrane.[36] Such systems show real promise for application in membrane transport. However, despite this potential, action of molecular motors in the membrane has not yet been studied in detail.

Herein, the design, synthesis, and study of the dynamic behavior of molecular motors under aqueous, physiologically relevant conditions is reported using two complementary strategies. First, two water-soluble, choline-modified molecular motors (first-generation motor **1** and second-generation motor **2**, Figure 1) were designed, and their isomerization processes

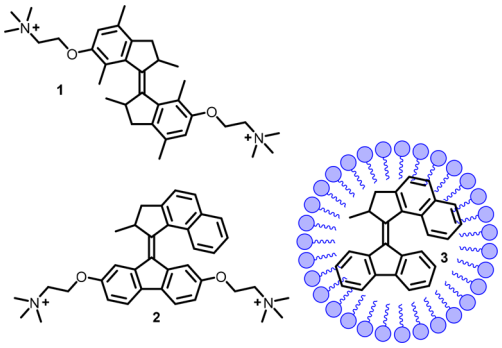

Figure 1. Structure of first-generation water-soluble motor **1**, second-generation water-soluble motor **2**, and second-generation motor **3** in micelles.

were studied in water. Second, molecular motor **3**, which is insoluble in water, was solubilized using micelles (Figure 1). Together, these two systems provide a basis for further research toward the application of molecular motors in biological systems.

RESULTS AND DISCUSSION

For the design of our water-soluble motor, we chose to functionalize a first-generation molecular motor with two quaternary ammonium groups. Scheme 1 shows the structure of this motor **1** and the typical rotation cycle for a first-generation molecular motor. On the basis of our previous

Scheme 1. Structure and Four-Step Rotation Cycle of Proposed Water-Soluble Motor 1 (counterions omitted for clarity)

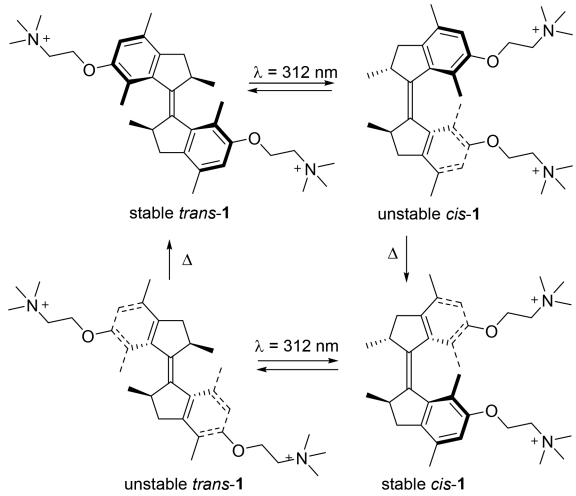

studies of rotary cycles of light-driven molecular motors,[18−22] we anticipated that starting from the stable trans isomer, irradiation causes photoisomerization of the central double bond, generating the unstable cis isomer. In this isomer, the methyl groups at the stereogenic centers are forced to assume an energetically unfavorable pseudoequatorial conformation. This steric strain is relieved in the irreversible thermal helix inversion (THI) step, upon which the stable cis isomer is formed. A second sequence of irradiation and thermal helix inversion leads to reformation of the stable trans isomer. After completion of the cycle, the top half of the motor has completed a 360° unidirectional rotation with respect to the lower half.

The synthesis of water-soluble motor **1** (Scheme 2) started from phenolic motor **4**, reported previously,[37] which was prepared in three steps on a multigram scale, and cis and trans isomers were separated using flash column chromatography. Dibromide-functionalized motor **5** was obtained in near quantitative yield using standard Williamson etherification in the presence of an excess of dibromoethane. Subsequent reaction with trimethylamine generated the quarternary ammonium salt **1**, which was easily purified by precipitation from the organic solution.

The rotational behavior of motor *trans*-**1** in water was investigated using ^{1}H NMR and UV−vis spectroscopies. Only the 180° rotation from stable trans to stable cis was studied. In the other half of the cycle (stable cis to stable trans), the half-life of the unstable trans isomer is expected to be <10 s at rt,[23] and therefore, this isomer is considered unsuitable to be studied in aqueous environment, which excludes the use of low-temperature measurements (below the freezing point of water). Figure 2 depicts the isomerization of stable *trans*-**1** in buffered D_2O (20 mM KPi, prepared by redissolving a lyophilized H_2O buffer at pH = 7.2, see SI page S2). For clarity, the aromatic hydrogen atoms and the methyl groups at the stereogenic centers are highlighted (for full spectra, see Figure S5). After 45 min irradiation at 312 nm, a ratio of ∼4:1 unstable cis/stable trans was determined. Irradiation was halted because several new signals appeared, indicative of minor degradation (Figure 2ii, boxes). Subsequently, the sample was left at rt for 5 days (Figure 2iii), and during this

DOI: 10.1021/acs.joc.8b01627
J. Org. Chem. 2018, 83, 11008−11018

Scheme 2. Synthesis of First-Generation Motor 1

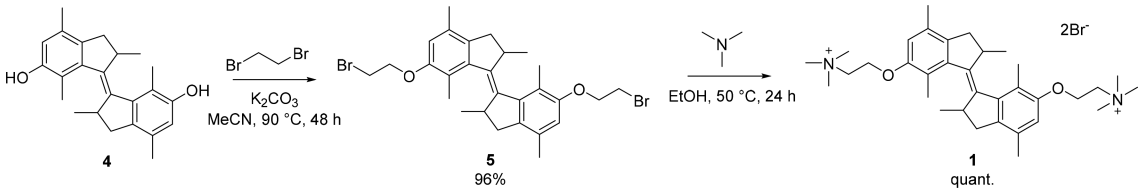

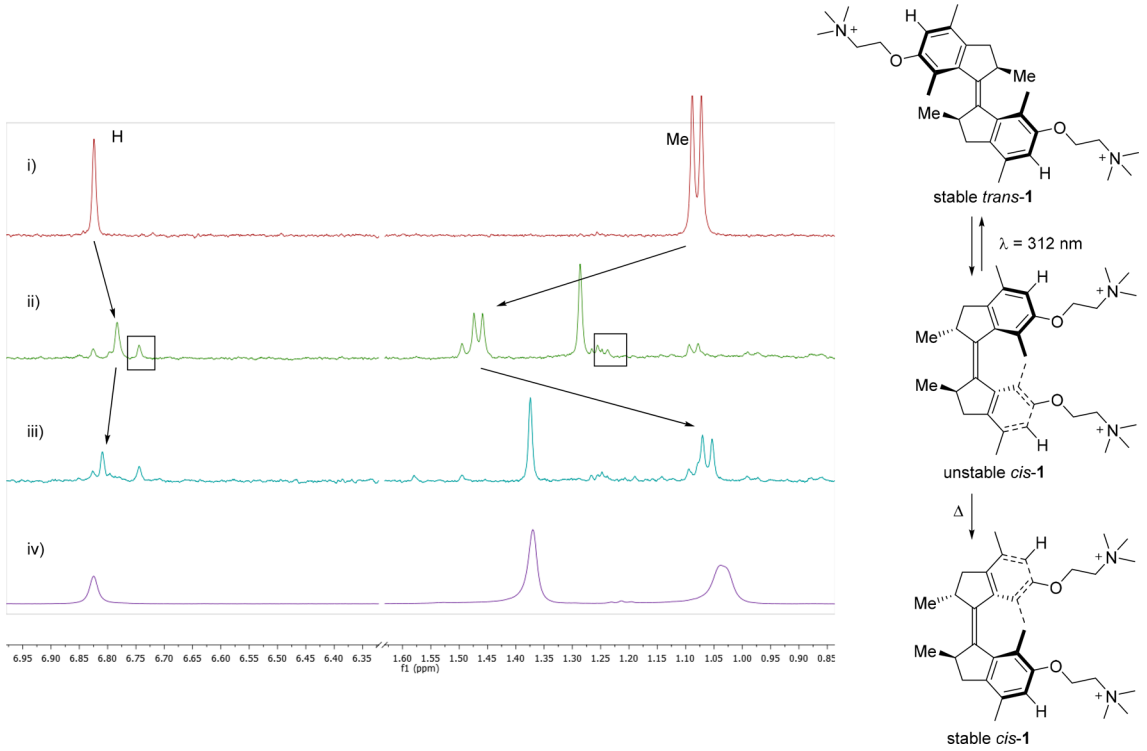

Figure 2. ^{1}H NMR experiments in buffered D_2O (20 mM KPi, pH = 7.2, 400 MHz, 20 °C, partial spectrum). (i) Stable *trans*-**1**. (ii) Sample after 45 min of irradiation (312 nm, 5 °C), showing also minimal degradation. (iii) Sample after 5 days at rt, consisting of a mixture of stable *cis*-**1** and , stable *trans*-**1**. (iv) Stable *cis*-**1**. Relevant peaks are indicated with arrows, unidentified side products with boxes. In spectra iii and iv, the signals of NMe_3 were aligned.

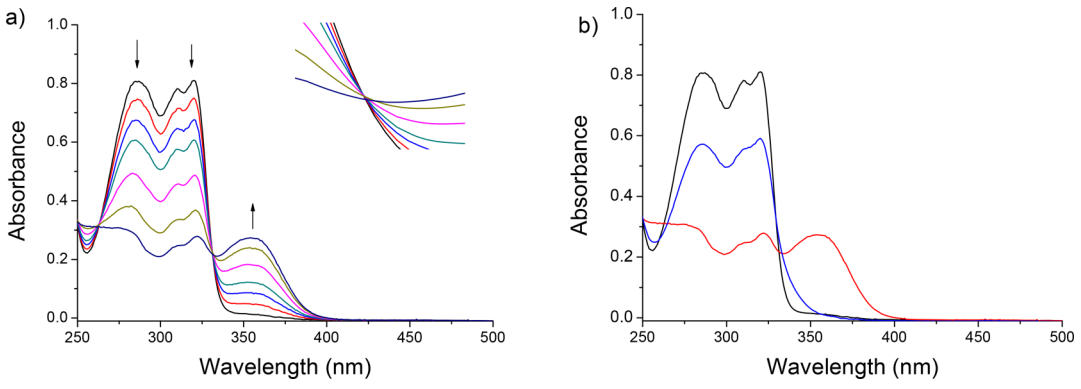

Figure 3. UV−vis analysis of the rotational behavior of motor **1** in PBS buffer (pH = 7.4). (a) Irradiation from stable *trans*-**1** (black line), 312 nm, 12 min, 20 °C. Inset shows the region 330−333 nm, 0.2−0.26 au. (b) Stable *trans*-**1** (black line), sample after 12 min of irradiation (red line), and after subsequent THI at room temperature overnight (blue line).

period all of the unstable cis isomer has converted to the stable cis isomer, and no additional degradation was observed.

The rotational process was subsequently studied using UV−vis spectroscopy. A solution of stable *trans*-**1** in PBS buffer (pH 7.4) was irradiated under air using λ = 312 nm UV light (Figure 3a). The appearance of a new band at higher wavelengths is indicative of the formation of the unstable cis isomer.[38] A clear isosbestic point at 330 nm indicates the absence of unwanted side reactions. After 12 min of irradiation, a slight isosbestic point shift was observed (Figure 3a, insert) and the irradiation was halted (Figure 3b, red line). The sample was subsequently left at room temperature overnight.

DOI: 10.1021/acs.joc.8b01627
J. Org. Chem. 2018, 83, 11008−11018

The new band at ~360 nm disappeared, and the band below 325 increased in absorption (Figure 3b, blue line). These changes are indicative of the THI and generation of the stable cis isomer.[39] By measuring the speed of the THI at various temperatures, an Eyring plot was constructed (see Figure S1) and the activation parameters of the unstable cis to stable cis conversion were calculated. The half-life of the unstable cis was found to be 22.8 h at rt and 18.5 min at body temperature (37 °C).

To complement the UV−vis and NMR measurements, the 180° rotation cycle from stable *trans*-**1** to stable *cis*-**1** was followed in aqueous PBS buffer (pH = 7.4) using CD spectroscopy. The *S,S*-enantiomer of stable *trans*-**4** was obtained through chiral resolution[37] and subsequently converted to stable *trans*-**1** using the same synthetic methodology as for the racemic motor (vide supra, Figure 2). Stable *trans*-*S,S*-**1** (Figure 4, black line) is enantiopure with a specific

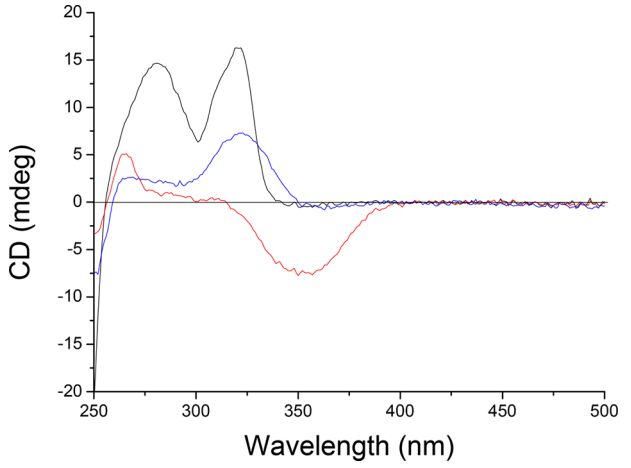

Figure 4. Circular dichroism spectra of isomers of motor **1** in PBS buffer (pH = 7.4). Stable *trans*-(*S,S*)-**1** (black line), PSS at 312 nm (red line) (unstable *cis*-(*S,S*)-**1**), and after THI at rt (blue line) (stable *cis*-(*S,S*)-**1**).

optical rotation ($[\alpha]^{20}_{D}$ = 51.2° (*c* 0.5, methanol)). After irradiation with λ = 312 nm light for 3 min, the photostationary state (PSS) was reached (Figure 4, red line). The higher wavelength CD band that is associated with formation of the unstable cis isomer showed a negative absorption, which is consistent with helicity inversion. After THI, the new band at 350 nm disappeared and a positive absorption at 325 nm was again observed, in accordance with a consecutive helicity inversion (Figure 4, blue line).

Molecular motor **1** appears to dissolve in aqueous media, since the absence of scattering effects at higher wavelengths (>450 nm) in the UV−vis spectrum (Figure 3) indicates that no aggregates are present in solution. However, due to the large aromatic core, motor **1** may behave as an amphiphile or bolaamphiphile at higher concentrations. The potential aggregation behavior of motor **1** was investigated using a fluorescence spectroscopy assay. Nile Red is a hydrophobic dye, which is poorly soluble in water and weakly fluoresces at around 660 nm.[40] In apolar environments, such as micelles or bilayers, the dye is soluble, which causes a strong increase in fluorescence and a blue shift of the emission spectrum. In Figure 5, the λ_{max} of the emission spectrum of Nile Red in the presence of both isomers of motor **1** is depicted. As expected, both isomers appear to be fully soluble at concentrations below

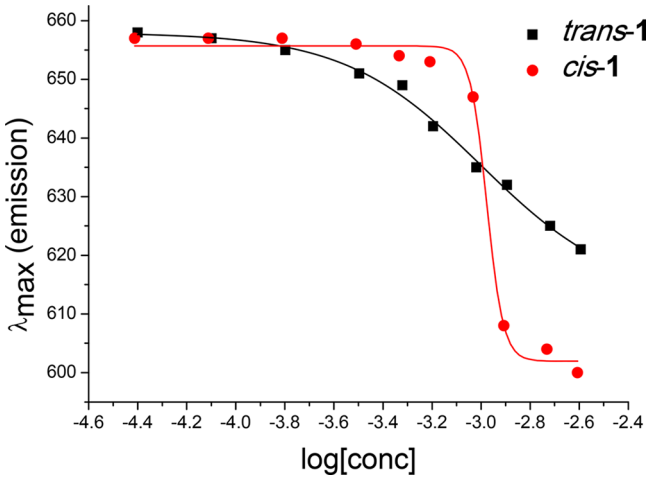

Figure 5. Emission of Nile Red in the presence of motor **1**, dissolved in aqueous buffer at pH = 10, λ_{ex} = 550 nm. Concentrations of **1** were varied between 40 μM and 2.5 mM; concentration of Nile red was ~1 μM for each sample.

0.1 mM, as demonstrated by the plateau around 660 nm. However, at higher concentrations, both isomers appear to aggregate, with a critical aggregation concentration of 1.0 mM for the cis isomer and 1.1 mM for the trans isomer. Notably, the sigmoidal curve is much steeper for the cis isomer than for the trans isomer. The reason for this difference is not clear, but the difference in aggregation behavior might be applied to create responsive aggregation at concentrations around 1.0 mM.

Using a combination of techniques, it has been established that new overcrowded alkene **1** is soluble in aqueous solution and functions as a molecular motor. However, the appearance of unidentified signals in the NMR spectrum (Figure 2) and a small isosbestic point shift in the UV−vis spectra (Figure 3) indicate that some minor degradation is occurring. To identify the nature of the degradation, several analytical techniques were used (see SI). From these results it can be concluded that motor **1** most probably undergoes water addition to the central double bond, which likely occurs in a photogenerated intermediate. Such a photoinduced water addition has previously been observed for dihydroquinolines.[41] By halting the irradiation at the moment that the PSS has been reached, degradation can be minimized and therefore does not pose a significant problem in potential future applications in aqueous media.

In contrast to the symmetric first-generation motors, second-generation motors are composed of two distinct halves, a stator and a rotor part.[20,42] This asymmetry facilitates synthetic modifications, for example, for surface anchoring, and allows for greater control over the rotation speed of the motor.[20,21,43] To expand our studies, we next investigated the behavior of second-generation motors under aqueous conditions. Our design was based on motor **3** (Figure 1), which exhibits excellent photochemical properties in organic solvents and a half-life of the unstable form of minutes, which is appropriate for study under ambient conditions.[44] In addition, derivatives of both the benzoindanone rotor and the fluorenone stator are generally readily accessible. The synthesis of water-soluble second-generation molecular motor **2** is outlined in Scheme 3. The synthesis of intermediate **9** has been reported previously,[45] but in the present study the motor was

DOI: 10.1021/acs.joc.8b01627
J. Org. Chem. 2018, 83, 11008−11018

Scheme 3. Synthesis of Second-Generation Motor 2

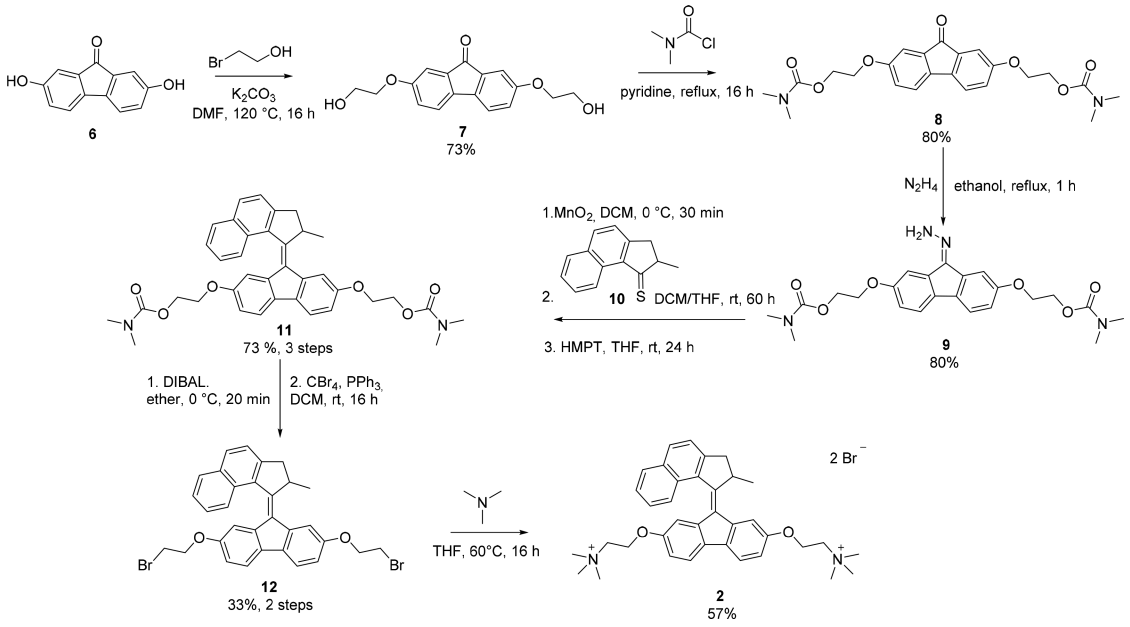

synthesized by a different, optimized route. Fluorenone **8** was prepared by a double Williamson etherification of commercially available dihydroxyfluorenone **6** with 2-bromoethanol to form disubstituted fluorenone **7**, followed by protection of the primary alcohol moieties with *N*,*N*-dimethyl carbamoyl chloride. After formation of hydrazone **9**, a Barton−Kellogg reaction was used to couple **9** to freshly prepared thioketone **10** to form overcrowded alkene **11**.[46] This motor was subjected to a DIBAL-mediated global deprotection, immediately followed by a double Appel reaction to give dibromo-functionalized motor **12**.[45] Synthesis of bis-ammonium-substituted motor **2** was completed by a double substitution using trimethylamine.

The switching behavior of motor **2** in water was studied with ^{1}H NMR spectroscopy. Figure 6 depicts the isomerization processes of the motor (PBS buffer, 1.9 mM, pH = 7.4; full spectra may be found in Figure S11). Stable **2** (Figure 6i) was irradiated with λ = 365 nm UV light for 16 h at 5 °C under air. The appearance of new peaks indicates formation of the unstable form. After 16 h, the PSS was reached, consisting of a ratio of unstable form/stable form of ∼1:2 (Figure 6ii). An improved PSS could be obtained by using methanol as solvent or cosolvent (see Figures S14 and S15). We were pleased to observe that the motor proved to be stable under irradiation in aqueous solution, with decomposition only observed upon prolonged irradiation (>3 days) (see Figure S12). Subsequently, the motor was left at room temperature for 8 h, and complete recovery of the original spectrum was observed, indicative of thermal isomerization to the stable form. It is interesting to note that slight shifts in the position of the NMR signals are observed. This effect is most likely due to the temperature dependence of chemical shifts or changes in aggregation as the concentration used is close to the critical aggregation constant.[47]

Subsequently, UV−vis spectroscopy was used to further probe the switching behavior. A solution of motor **2** in PBS buffer was irradiated with a λ = 385 nm LED (Figure 7a). A broadening of the signal and a shift toward higher wavelengths was observed, as well as a clear isosbestic point, characteristic

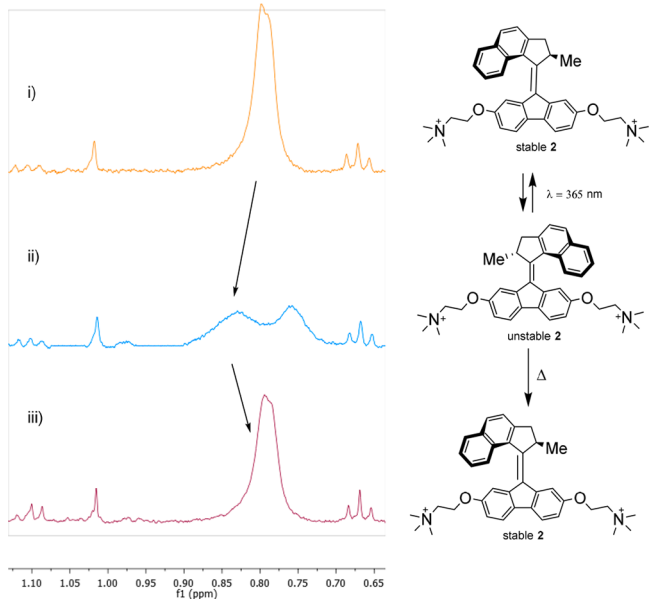

Figure 6. ^{1}H NMR experiments in buffered D_2O (20 mM KPi, pH = 7.4, 400 MHz, 20 °C). (i) Stable **2**. (ii) Sample after 3 days of irradiation (365 nm, 5 °C). (iii) Sample after 3 days at rt, consisting of stable **2**. Relevant Me peaks are indicated with arrows.

of a selective transition to the unstable form.[21] After 15 min, no further changes were observed in the spectrum and irradiation was halted (Figure 7b). After leaving the sample at room temperature, complete regeneration of the initial spectrum was observed, indicating thermal isomerization to the stable form (Figure 7b). Subsequently, the rate of the THI was recorded at different temperatures. Using these data, an Eyring analysis was performed and the activation parameters were determined (see Table S2 and Figure S9). The half-life was found to be 47 min at room temperature and 7.5 min at 37 °C. Finally, UV−vis spectroscopy was used to evaluate the fatigue resistance of the motor (Figure 7c). The motor was irradiated with a λ = 385 nm LED and then left at 37 °C for 1.5

DOI: 10.1021/acs.joc.8b01627
J. Org. Chem. 2018, 83, 11008−11018

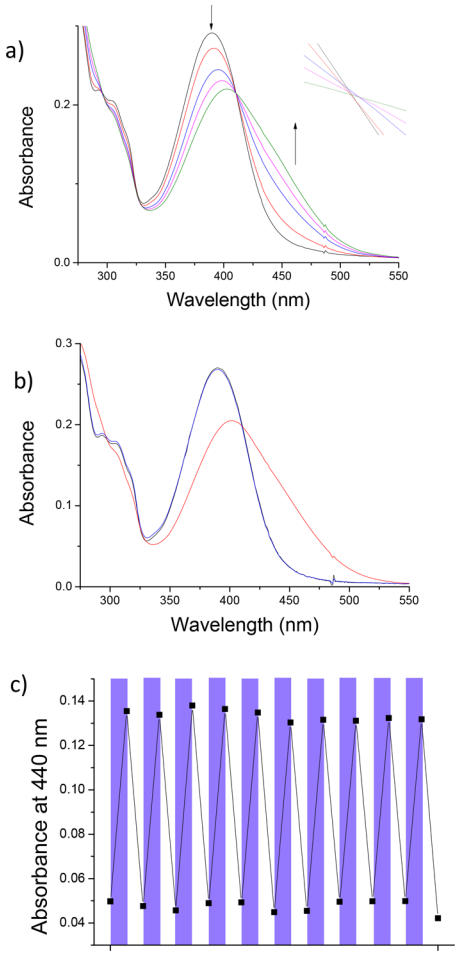

Figure 7. UV−vis analysis of the rotational behavior of motor **2** in PBS buffer (pH = 7.4). (a) Irradiation from stable **2** (black line), 385 nm, 15 min, 20 °C. Inset shows the isosbestic point in the region 409−412 nm, 0.21−0.22 au. (b) Stable **2** (black line), sample after 15 min of irradiation (red line), and after subsequent THI at room temperature for 6 h (blue line). (c) Fatigue resistance experiment of motor **2** in aqueous buffer (pH = 7.4). Absorbance at 440 nm was monitored after each irradiation with 385 nm light (15 min, purple bands) or THI (37 °C, 1.5 h, white bands).

h. No noticeable change in UV−vis absorption was observed over 10 switching cycles, demonstrating the high fatigue resistance of motor **2** under aqueous conditions.

While the lack of scattering effects in the UV−vis spectrum indicates that no aggregation occurs at low micromolar concentrations, the hydrophobic core of the motor has a potential for aggregation, as observed for motor **1**. The aggregation behavior was investigated using a fluorescence spectroscopy assay. The wavelength of the emission maximum of the Nile Red fluorescence was measured and used to determine the critical aggregation constant, which was found to be 1.1 mM, very similar to motor **1** (Figure 8). This suggests that the adopted synthetic modification is general and can be used for enabling water solubility at biologically relevant submillimolar concentrations.

Water-soluble motors may find application both inside and outside of the cell. Complementary to these, applications may be envisioned in which molecular motors need to operate in the biological membrane. All motors reported by our group thus far are only soluble in organic solvents, with the exception

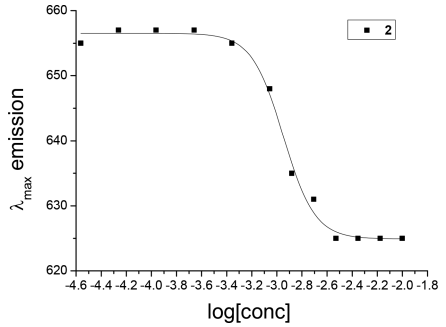

Figure 8. λ_{max} of the emission of Nile Red in the presence of varying concentrations of motor **2**, dissolved in Milli-Q. λ_{ex} = 550 nm. Concentration of motor **2** was varied between 25 μM and 10 mM, while the Nile Red fluorescent dye concentration was kept constant at ∼2 μM by addition of a 1 mM ethanol stock solution.

of a recent system that was shown to aggregate in water.[27] In theory, many of these may also be operated in a bilayer, which provides a hydrophobic environment. To study the operation of molecular motors for potential use in the cell membrane, a model system was designed. Molecular motor **3** (Scheme 4)

Scheme 4. Motor 3 and Its Rotary Cycle

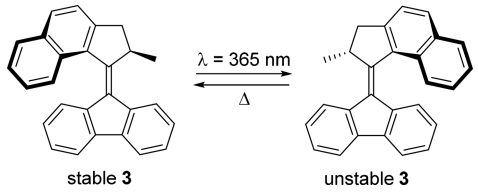

has excellent photochemical properties, with high photostationary states and a half-life of the unstable isomer of 3.17 min at rt in hexane.[44] To mimic conditions in a bilayer, motor **3** was encapsulated in micelles. Sodium dodecyl sulfate (SDS) was used as the surfactant (CMC = 8.5 mM in water).

The rotational properties of motor **3** in the presence of SDS micelles were studied using UV−vis spectroscopy. Initially, the quality of the UV−vis spectrum was rather poor, with no defined absorption bands and absorbance up to 900 nm (Figure 9a, black line). However, after 16 h at rt, a sharper absorption band could be observed (λ_{max} = 388 nm, Figure 9a, red line), which was very similar to the absorbance of **3** in hexane (λ_{max} ≈ 390 nm). The absorbance at higher wavelengths, seen initially, may be attributed to scattering effects of larger aggregates of **3**. The disappearance of the scattering is indicative of solubilization of **3** in the micelles. Irradiation with λ = 365 nm light led to the formation of a new, broader absorption band at a higher wavelength (λ_{max} = 411 nm, Figure 9a, blue line), again similar to the absorption corresponding to the unstable isomer in hexane (λ_{max} ≈ 420 nm).[44] The clear isosbestic point that can be observed at λ = 406 nm (Figure 9b) is indicative of a lack of side reactions. After leaving the sample at rt for 1 h, the initial spectrum is regenerated (Figure 9a, turquoise line), indicating a complete THI to stable **3**. Eyring analysis of the THI revealed that the half-life of **3** in micelles is 4.93 min, somewhat longer than in hexane (3.17 min). See SI (Table S3 and Figure S16) for full Eyring analysis and activation parameters. The stability of motor **3** in micelles in aqueous buffer solution was further investigated by operating the motor over a pH range (see Figure S18). Switching function of the motor was retained in

DOI: 10.1021/acs.joc.8b01627
J. Org. Chem. 2018, 83, 11008−11018

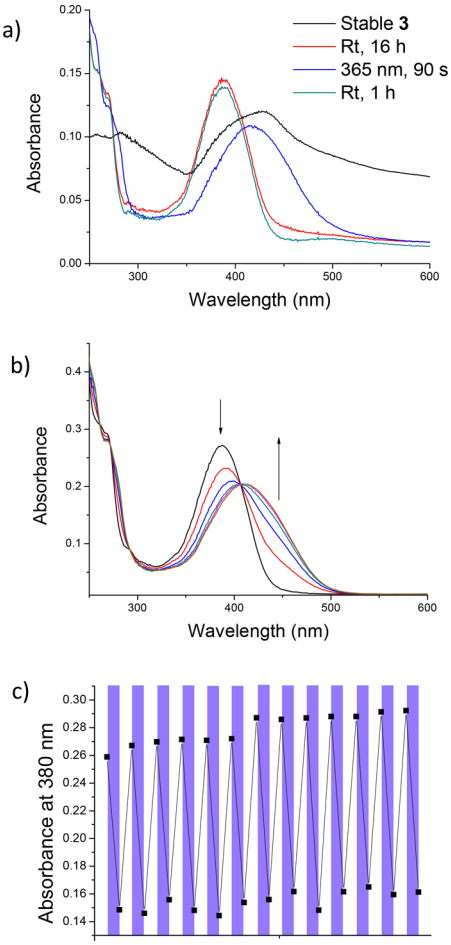

Figure 9. UV−vis spectra of motor **3** in buffer (25 mM Tris, Bis-Tris, MES, and sodium acetate, pH= 7.4) in the presence of SDS. (a) Motor **3** (black line), sample after 16 h (red line), PSS (blue line), and after THI (turquoise line). (b) Motor **3** upon irradiation with 365 nm light. All spectra recorded at 20 °C under ambient atmosphere. (c) Fatigue resistance experiment of motor **3** in buffer (pH = 7.4) and 20 mM SDS. Absorbance at 380 nm was monitored after each irradiation with 365 nm light (1 min, purple bands) or THI (rt, 1 h, white bands). Due to duration of the experiment, the sample was left at rt overnight, which accounts for the small baseline shift observed between cycles 6 and 7.

samples ranging from at pH = 2 to pH = 10, even after up to 1 week of incubation at rt.

To confirm that the motor is actually dissolved in micelles, the UV−vis experiment was repeated in PBS buffer only (pH = 7.4). Although some switching behavior could be observed in aqueous buffer without SDS (see Figure S17), the motor is likely not solubilized, which impedes its function. Upon irradiation and subsequent THI of motor **3** in 20 mM SDS in buffer (25 mM Tris, Bis-Tris, MES and sodium acetate, pH = 7.4), no degradation of the motor was observed Figure 9b). As observed previously (vide supra), the central double bond of a molecular motor can be vulnerable to water addition in aqueous environments. Incorporation of the motor in micelles appears to solve this issue. Irradiation with 365 nm light and subsequent THI were repeated for 13 cycles to investigate fatigue resistance of **3** in micelles (Figure 9c). From these experiments, it is evident that the system is shown to be highly fatigue resistant in aqueous buffer solution.

The combined results of these UV−vis experiments indicate that **3** can be fully solubilized in a micelle at micromolar concentration. It is expected that this holds for many other, similar molecular motors. The motor also shows to be highly fatigue resistant under these conditions. These findings provide an excellent basis for future studies aiming at the performance of molecular motors in the cellular membrane.

CONCLUSIONS

In summary, the functioning of molecular motors in two biologically relevant media, aqueous buffer and micelles, was demonstrated. For this purpose, first- and a second-generation motors containing solubilizing ammonium substituents were synthesized. Both motors were found to be soluble in water and only aggregated at millimolar concentrations. The switching cycle was followed by NMR, UV−vis, and CD spectroscopy, and the compounds were demonstrated to display the typical behavior of light-driven molecular motors. Minor degradation was observed for first-generation molecular motor **1**, which was attributed to water addition across the double bond. In contrast, a related second-generation motor **2** was shown to be perfectly stable while undergoing rotary motion in aqueous solution. Furthermore, second-generation motor **3** was employed in micelles to mimic cell membranes and other hydrophobic environments. The photo- and thermochemical behavior of this motor in the micelles was similar to the motor dissolved in hexane and the motor proved to be stable under irradiation. Together, these experiments demonstrate the potential of molecular motors to be employed as photoswitches and molecular machines for applications in various aqueous systems. With their four-state switching cycle, unidirectional rotation, and switching chirality, molecular motors offer precision and control beyond the properties of conventional photoswitches and pave the way for novel responsive biological systems and innovative applications in photopharmacology and biological nanotechnology.

EXPERIMENTAL SECTION

General Information. Chemicals were purchased from Sigma-Aldrich, Acros, or TCI Europe N.V. and were used without prior purification. Dry solvents were obtained from an MBraun solvent purification system. Column chromatography was performed on silica gel (Silica Flash P60, 230−400 mesh). TLC: silica gel 60, Merck, 0.25 mm. HRMS spectra were recorded on a Thermo Fischer Scientific Orbitrap XL with ESI, APPI, and/or APCI ionization sources. Deuterated buffered solutions were prepared from buffered solutions of a known pH, which were subjected to three cycles of freeze−drying and subsequent redissolving in D_2O. ^1H and ^{13}C NMR were recorded on a Varian Gemini-200 (^1H 200 MHz, ^{13}C 50 MHz), a Varian AMX400 (^1H 400 MHz, ^{13}C 101 MHz), or a Varian Unity Plus (^1H 500 MHz, ^{13}C 125 MHz) at room temperature unless otherwise stated. Chemical shifts are denoted in δ values (ppm) relative to $CDCl_3$ (^1H δ = 7.26 and ^{13}C δ = 77.16), CD_2Cl_2 (^1H δ = 5.32 and ^{13}C δ = 53.84), DMSO (^1H δ = 2.50 and ^{13}C δ = 39.52), MeOD (^1H δ = 3.31 and ^{13}C δ = 49.00), or D_2O (^1H δ = 4.79). For ^1H NMR, the splitting parameters are designated as follows: s (singlet), d (doublet), t (triplet), q (quartet), p (pentet), h (heptet), m (multiplet), bs (broad singlet), and app (apparent). Unless otherwise stated, all measurements were performed on racemic mixtures. Melting points were taken on a Büchi B-545 melting point apparatus. CD spectra were recorded on a JASCO J-810 spectropolarimeter. UV−vis absorption spectra were measured on a Jasco V-630 spectrometer in 1 cm quartz cuvettes. Irradiation was performed using a Spectroline ENB-280C/FE lamp (312 or 365 nm) or a LED (5 W, 365 or 385 nm, 10 nm width at half-height).

DOI: 10.1021/acs.joc.8b01627
J. Org. Chem. 2018, 83, 11008−11018

*2,2′,4,4′,7,7′-Hexamethyl-2,2′,3,3′-tetrahydro-[1,1′-biindenylidene]-6,6′-diol (**4**).* Motor **4** was synthesized according to a previously reported procedure.[37] The product was obtained as a yellow solid. (496 mg, 1.43 mmol, 96%). Enantiomers could be separated using chiral resolution.[37] **Trans**: ^{1}H NMR (400 MHz, CD_3OD) δ 6.49 (s, 2H), 2.86 (app. p, 2H), 2.51 (dd, J = 14.1, 5.6 Hz, 2H), 2.25 (s, 6H), 2.15 (d, J = 14.1 Hz, 2H), 2.10 (s, 6H), 1.08 (d, J = 6.4 Hz, 6H). ^{13}C NMR (101 MHz, CD_3OD) δ 155.3, 143.5, 142.8, 133.9, 132.6, 119.4, 115.2, 43.4, 39.1, 19.7, 18.4, 16.5. mp = 235.5 °C. **Cis**: ^{1}H NMR (400 MHz, CD_3OD) δ 6.50 (s, 2H), 3.38−3.29 (m, 2H, overlap with solvent peak), 3.01 (dd, J = 14.4, 6.2 Hz, 2H), 2.40 (d, J = 14.4 Hz, 2H), 2.20 (s, 6H), 1.38 (s, 6H), 1.07 (d, J = 6.7 Hz, 6H). ^{13}C NMR (101 MHz, CD_3OD) δ 154.7, 143.3, 142.0, 136.2, 131.9, 121.2, 115.6, 43.2, 39.0, 20.8, 18.5, 14.5. mp = 218−219 °C. HRMS (ESI) m/z: $[M + 1]^+$ Calcd for $C_{24}H_{29}O_2$ 349.2162; Found 349.2160.

*6,6′-Bis(2-bromoethoxy)-2,2′,4,4′,7,7′-hexamethyl-2,2′,3,3′-tetrahydro-1,1′-biindenylidene (**5**).* **Trans**: Overcrowded alkene **4** (107 mg, 0.307 mmol) was dissolved in acetonitrile (10 mL). K_2CO_3 (1.06 g, 7.69 mmol) and 1,2-dibromoethane (67 μL, 0.77 mmol) were added, and the mixture was heated to 90 °C for 48 h. The reaction mixture was cooled to room temperature, and water (20 mL) was added. The mixture was extracted with ethyl acetate (3 × 15 mL), and the combined organic layers were subsequently washed with brine (15 mL), dried over $MgSO_4$, and concentrated in vacuo. No further purification was necessary. **Trans**: Overcrowded alkene **5** was obtained as a brown solid (107 mg, 0.226 mmol, 74% yield). **Cis**: overcrowded alkene **5** could be obtained in an analogous manner. **Cis**: ^{1}H NMR (400 MHz, $CDCl_3$) δ 6.53 (s, 2H), 4.25 (app. ddt, 4H), 3.62 (t, J = 6.3 Hz, 4H), 3.34 (app. p, 6H), 3.05 (dd, J = 14.6, 6.3 Hz, 6H), 2.39 (d, J = 14.6 Hz, 6H), 2.25 (s, 6H), 1.41 (s, 6H), 1.07 (d, J = 6.7 Hz, 6H). ^{13}C NMR (101 MHz, $CDCl_3$) δ 155.1, 142.5, 141.2, 137.3, 130.9, 123.1, 112.9, 69.1, 42.0, 38.3, 30.1, 20.6, 19.0, 14.5. mp = 151.8 °C. **Trans**: ^{1}H NMR (400 MHz, $CDCl_3$) δ 6.53 (s, 2H), 4.31 (app. ddt, 4H), 3.71 (t, J = 6.2 Hz, 4H), 2.86 (app. p, 2H), 2.60 (dd, J = 14.2, 5.7 Hz, 2H), 2.33 (s, 6H), 2.18 (app. m, 8H), 1.09 (d, J = 6.4 Hz, 6H). ^{13}C NMR (101 MHz, $CDCl_3$) δ 155.5, 142.8, 141.9, 135.1, 131.6, 121.1, 111.7, 68.7, 42.4, 38.5, 30.1, 19.4, 18.9, 16.4. mp = 151−152 °C. HRMS (ESI) m/z: $[M + 1]^+$ Calcd for $C_{28}H_{35}Br_2O_2$ 563.0978, Found 563.0964.

*2,2′-((2,2′,4,4′,7,7′-Hexamethyl-2,2′,3,3′-tetrahydro-[1,1′-biindenylidene]-6,6′-diyl)bis(oxy))bis(N,N,N-trimethylethan-1-aminium) (**1**).* Molecular motor *trans*-**5** (49 mg, 0.087 mmol) was mixed with a 4.3 M NMe_3 solution in ethanol (4.0 mL, 17 mmol) in a pressure tube. The tube was closed and stirred overnight at 50 °C. After cooling down to room temperature, diethyl ether (20 mL) was added to the reaction mixture. The precipitate was filtered off, and *trans*-**1** was obtained as a light brown solid in quantitative yield (59 mg, 0.087 mmol). *cis*-**1** could be obtained in analogous manner. **Cis**: ^{1}H NMR (400 MHz, D_2O) δ 6.76 (s, 2H), 4.42 (app. d, 4H), 3.81 (app. s, 4H), 3.33 (app. d, J = 19.5 Hz, 2H), 3.20 (s, 18H), 2.95 (d, J = 14.3 Hz, 2H), 2.39 (d, J = 15.2 Hz, 2H), 2.31 (s, 6H), 1.30 (s, 6H), 0.97 (d, J = 6.1 Hz, 6H). ^{13}C NMR (101 MHz, D_2O) δ 156.9, 145.2, 144.2, 140.7, 134.7, 124.1, 113.9, 68.1, 65.0, 56.6, 44.4, 40.0, 21.9, 20.2, 16.3. mp > 310 °C (dec). **Trans**: ^{1}H NMR (400 MHz, D_2O) δ 6.78 (s, 2H), 4.49 (app. d, 4H), 3.89 (app. s, 4H), 2.77 (app. t, 2H), 2.43 (app. d, 2H), 2.29 (s, 6H), 2.22 (d, J = 14.8 Hz, 2H), 2.16 (s, 6H), 1.03 (d, J = 6.3 Hz, 6H). ^{13}C NMR (101 MHz, D_2O) δ 157.5, 145.0, 144.5, 137.9, 135.1, 122.9, 113.8, 68.1, 65.0, 56.7, 44.4, 39.8, 20.8, 20.0, 18.4. mp > 240 °C (dec). HRMS (ESI) m/z: $M2^+$ Calcd for $C_{34}H_{52}N_2O_2$ 260.2009; Found 260.2005.

*2,7-Bis(2-hydroxyethoxy)-9H-fluoren-9-one (**7**).* Potassium carbonate (2.64 g, 19.1 mmol), 2,7-dihydroxyfluorenone **6** (984 mg, 4.64 mmol), and 2-bromoethanol (2.00 mL, 28.2 mmol) were suspended in anhydrous DMF (15 mL), and the mixture was heated at 120 °C for 16 h under a nitrogen atmosphere. After cooling to rt, the volatiles were removed under vacuum and the solid residue was washed with water (100 mL). The crude solid was recrystallized from ethanol. Product **7** was obtained as a red powder (1.01 g, 3.38 mmol, 73%). ^{1}H NMR (400 MHz, DMSO-d_6) δ 7.56 (d, J = 8.8 Hz, 2H), 7.10−7.08 (m, 4H), 4.89 (br. s, 2H), 4.05 (t, J = 4.8 Hz, 4H), 3.71 (t, J = 4.6 Hz, 4H). ^{13}C NMR (101 MHz, DMSO-d_6) δ 192.8, 159.1, 136.8, 135.1, 121.5, 120.9, 110.1, 70.1, 59.5. mp = 145−147 °C. HRMS (ESI) m/z: $[M + 1]^+$ Calcd for $C_{17}H_{17}O_5$ 301.1071, Found 301.1070.

*((9-Oxo-9H-fluorene-2,7-diyl)bis(oxy))bis(ethane-2,1-diyl) bis(dimethylcarbamate) (**8**).* Fluorenone **7** (5.98 g, 19.9 mmol) was dissolved in pyridine (60 mL). Dimethylcarbamoyl chloride (16.0 mL, 174 mmol) was slowly added, and the solution was heated at reflux for 16 h under a nitrogen atmosphere. The mixture was cooled to room temperature and carefully poured on ice (200 g). The mixture was extracted with DCM (3 × 100 mL), and the combined organic layers were dried over $MgSO_4$. The volatiles were removed in vacuo, and the crude product was recrystallized from ethanol (30 mL) to give the product **8** as an orange powder (6.65 g, 15.9 mmol, 80%). ^{1}H NMR (500 MHz, $CDCl_3$, performed at −25 °C to resolve the rotamers of the carbamate) δ 7.29 (app. t, 2H), 7.17−7.09 (m, 2H), 6.99−6.90 (m, 2H), 4.44−4.40 (m, 4H), 4.21−4.17 (m, 4H), 2.94 (s, 6H), 2.92 (s, 6H). ^{13}C NMR (126 MHz, $CDCl_3$, performed at −25 °C to resolve the rotamers of the carbamate) δ 193.9, 158.8, 156.2, 137.5, 135.6, 120.8, 110.1, 77.2, 66.6, 63.6, 36.5, 36.0. mp = 126−128 °C. HRMS (ESI) m/z: $[M + 1]^+$ Calcd for $C_{23}H_{27}N_2O_7$ 443.1813; Found 443.1806.

*((9-Hydrazineylidene-9H-fluorene-2,7-diyl)bis(oxy))bis(ethane-2,1-diyl) bis(dimethylcarbamate) (**9**).* Ethanol (50 mL) was degassed with a flow of nitrogen for 1 h. Carbamate **8** (5.96 g, 14.2 mmol) and hydrazine hydrate (15 mL) were added, and the solution was heated at reflux for 1 h under a nitrogen atmosphere. Water (100 mL) was added, and the solution was slowly cooled to rt. The mixture was filtered under vacuum, and the crude product was washed with water and dried under vacuum to give the product **9** as a yellow powder (4.91 g, 11.3 mmol, 80%). ^{1}H NMR (500 MHz, $CDCl_3$, performed at −25 °C to resolve the rotamers of the carbamate) δ 7.52 (d, J = 8.3 Hz, 1H), 7.47 (s, 1H), 7.43 (d, J = 8.3 Hz, 1H), 7.20 (s, 1H), 6.89 (app. t, 2H), 6.42 (br. s, 2H), 4.46−4.37 (m, 4H), 4.21 (app. s, 4H), 2.92 (s, 3H), 2.91 (s, 3H), 2.90 (s, 3H), 2.89 (s, 3H). ^{13}C NMR (126 MHz, $CDCl_3$, performed at −25 °C to resolve the rotamers of the carbamate) δ 158.2, 157.6, 156.4, 156.3, 145.2, 139.0, 134.3, 131.8, 131.2, 120.3, 120.0, 116.1, 114.2, 113.4, 105.4, 66.6, 66.5, 63.8, 63.6, 36.5, 36.5, 36.1, 36.0. mp = 85−87 °C. HRMS (ESI) m/z: $[M + 1]^+$ Calcd for $C_{23}H_{29}N_4O_6$ 457.2082; Found 457.2077.

*((9-(2-Methyl-2,3-dihydro-1H-cyclopenta[a]naphthalen-1-ylidene)-9H-fluorene-2,7-diyl)bis(oxy))bis(ethane-2,1-diyl) bis(dimethylcarbamate) (**11**).* Hydrazone **9** (3.36 g, 7.78 mmol) was dissolved in anhydrous DCM (30 mL) and cooled to 0 °C. Activated manganese dioxide (5.11 g, 58.8 mmol) was added, and the reaction was followed by TLC until completion (5% MeOH in DCM). After filtration through Celite, freshly prepared thioketone **10** (1.94 g, 9.16 mmol) was added in anhydrous THF (30 mL).[46] The solution was stirred at room temperature for 60 h under a nitrogen atmosphere. A solution of HMPT (1.36 mL, 7.48 mmol) in anhydrous THF (20 mL) was added, and the mixture was stirred for 24 h under a nitrogen atmosphere. The volatiles were removed under vacuum, and the crude product was purified by column chromatography (pentane:ethyl acetate, 50:50 to 30:70) to give the product **11** as an orange powder (3.31 g, 5.67 mmol, 73%). ^{1}H NMR (500 MHz, $CDCl_3$, performed at −25 °C to resolve the rotamers of the carbamate) δ 7.94 (app. t, 2H), 7.75 (d, J = 8.3 Hz, 1H), 7.63 (d, J = 8.3 Hz, 1H), 7.60 (d, J = 8.2 Hz, 1H), 7.53 (d, J = 8.3 Hz, 1H), 7.51−7.48 (m, 1H), 7.45 (t, J = 7.2 Hz, 1H), 7.38 (t, J = 7.2 Hz, 1H), 6.95 (dd, J = 8.3, 1.9 Hz, 1H), 6.80 (dd, J = 8.2, 2.2 Hz, 1H), 6.22 (d, J = 2.0 Hz, 1H), 4.54−4.46 (m, 2H), 4.35−4.23 (m, 3H), 4.05−3.95 (m, 2H), 3.55 (dd, J = 15.1, 5.4 Hz, 1H), 3.28−3.23 (dd, J = 17.2, 2.9 Hz, 1H), 2.96−2.91 (m, 7H), 2.88 (s, 3H), 2.80−2.75 (m, 4H), 1.40 (d, J = 6.7 Hz, 3H). ^{13}C NMR (126 MHz, $CDCl_3$, performed at −25 °C to resolve the rotamers of the carbamate) δ 157.5, 156.4, 156.2, 151.5, 147.7, 140.9, 137.8, 135.8, 133.5, 132.9, 132.3, 131.2, 130.1, 129.4, 128.9, 127.6, 126.7, 125.2, 124.2, 119.5, 119.0, 115.7, 112.8, 111.1, 110.4, 66.7, 65.4, 64.0, 63.6, 45.1, 41.8, 36.5, 36.4, 36.1, 35.9, 19.3. mp = 57−59 °C. HRMS (ESI) m/z: $[M + 1]^+$ Calcd for $C_{37}H_{39}N_2O_6$: 607.2803; Found 607.2790.

DOI: 10.1021/acs.joc.8b01627
J. Org. Chem. 2018, 83, 11008−11018

*2,7-Bis(2-bromoethoxy)-9-(2-methyl-2,3-dihydro-1H-cyclopenta-[a]naphthalen-1-ylidene)-9H-fluorene (**12**).* A flame-dried flask was charged with motor **11** (2.01 g, 3.31 mmol) and anhydrous diethyl ether (115 mL), and the mixture was cooled to 0 °C under a nitrogen atmosphere. DIBAL-H (1.2 M in THF, 13.7 mL, 16.5 mmol) was slowly added over 5 min, and the mixture was stirred at 0 °C for 20 min. The solution was poured on ice (200 g) and extracted with ethyl acetate (3 × 200 mL). The combined organic layers were dried over $MgSO_4$. After removal of the volatiles in vacuo the crude product was purified by column chromatography (MeOH:DCM, 2:98 to 3:97). The double primary alcohol functionalized product was reported to be unstable and was therefore immediately used in the subsequent step.[45] The product was dissolved in anhydrous DCM (100 mL) and added to a flame-dried flask. The solution was cooled to 0 °C, and carbon tetrabromide (3.33 g, 10.1 mmol) was added. Subsequently, triphenyl phosphine (2.63 g, 9.92 mmol) was slowly added, and the solution was stirred for 16 h. The volatiles were removed under vacuum, and the crude product was purified by column chromatography (pentane:DCM 85:15) to give product **12** as an orange powder (636 mg, 1.08 mmol, 33% from **10**). ^{1}H NMR (400 MHz, $CDCl_3$) δ 7.99−7.89 (m, 2H), 7.75 (d, J = 8.3 Hz, 1H), 7.62 (d, J = 8.3 Hz, 1H), 7.59 (d, J = 8.2 Hz, 1H), 7.55−7.50 (m, 2H), 7.47 (t, J = 7.5 Hz, 1H), 7.37 (t, J = 8.1 Hz, 1H), 6.94 (dd, J = 8.3, 2.2 Hz, 1H), 6.79 (dd, J = 8.3, 2.3 Hz, 1H), 6.21 (d, J = 2.2 Hz, 1H), 4.41 (t, J = 6.4 Hz, 2H), 4.31 (app. p, 1H), 3.71 (t, J = 6.4 Hz, 2H), 3.58 (dd, J = 15.2, 5.6 Hz, 1H), 3.44−3.37 (m, 1H), 3.27−3.08 (m, 3H), 2.78 (d, J = 15.2 Hz, 1H), 1.41 (d, J = 6.7 Hz, 3H). ^{13}C NMR (101 MHz, $CDCl_3$) δ 157.3, 156.4, 151.7, 147.7, 141.3, 138.4, 136.1, 134.4, 133.6, 132.8, 131.3, 130.4, 129.8, 129.1, 127.7, 126.9, 125.5, 124.3, 119.7, 119.3, 116.3, 113.8, 111.9, 111.3, 68.8, 67.6, 45.3, 42.1, 29.4, 29.3, 19.4. mp = 77−78 °C. HRMS (ESI) m/z: $[M + 1]^+$ Calcd for $C_{31}H_{27}Br_2O_2$ 591.0352; Found 591.0341.

*2,2′-((9-(2-Methyl-2,3-dihydro-1H-cyclopenta[a]naphthalen-1-ylidene)-9H-fluorene-2,7-diyl)bis(oxy))bis(N,N,N-trimethylethan-1-aminium) (**2**).* Motor **12** (203 mg, 3.44 mmol) was added to a 2 M NMe_3 solution in THF (15.0 mL, 30.0 mmol) in a pressure tube and heated at 60 °C for 16 h. The mixture was cooled to room temperature, and ether was added (15 mL). The suspension was filtered under vacuum. The crude solid was recrystallized twice from an ethyl acetate and ethanol mixture (ethanol:ethyl acetate, 25:75) to give the product **2** as a yellow powder (139 mg, 1.97 mmol, 57%). ^{1}H NMR (400 MHz, CD_3OD) δ 8.03 (d, J = 8.3 Hz, 2H), 7.63 (d, J = 8.2 Hz, 1H), 7.49 (d, J = 8.3 Hz, 1H), 7.44 (t, J = 7.6 Hz, 1H), 7.32 (d, J = 8.3 Hz, 1H), 7.27 (d, J = 8.3 Hz, 1H), 7.23 (s, 1H), 7.01 (t, J = 7.5 Hz, 1H), 6.93 (d, J = 8.2 Hz, 1H), 6.62 (dd, J = 8.3, 1.9 Hz, 1H), 5.81 (d, J = 1.8 Hz, 1H), 4.53−4.37 (m, 2H), 3.96 (app. p, 6.2 Hz, 1H), 3.79 (t, J = 4.8 Hz, 2H), 3.52−3.41 (m, 1H), 3.27−3.23 (m, 11 H), 3.15−3.07 (m, 1H), 2.87 (s, 9H), 2.67 (d, J = 16.7 Hz, 1H), 1.10 (d, J = 6.6 Hz, 3H). ^{13}C NMR (101 MHz, CD_3OD) δ 158.1, 156.8, 153.1, 149.4, 142.3, 139.6, 136.8, 135.5, 135.3, 134.2, 132.7, 131.1, 130.9, 130.3, 128.6, 127.7, 126.5, 125.5, 121.0, 120.4, 115.3, 114.7, 113.2, 112.2, 66.8, 66.1, 63.7, 62.8, 54.9, 54.7, 46.3, 42.8, 19.4. mp > 210 °C (dec). HRMS (ESI) m/z: $M2^+$ Calcd for $C_{37}H_{44}N_2O_2$ 274.1696; Found 274.1700.

■ ASSOCIATED CONTENT

Supporting Information

The Supporting Information is available free of charge on the ACS Publications website at DOI: 10.1021/acs.joc.8b01627.

Analytical data of all title compounds (^{1}H NMR, ^{13}C NMR), Eyring plot analysis, UV−vis spectra, NMR experiments (PDF)

■ AUTHOR INFORMATION

Corresponding Authors

*w.szymanski@umcg.nl

*b.l.feringa@rug.nl

ORCID

Wiktor Szymanski: 0000-0002-9754-9248

Ben L. Feringa: 0000-0003-0588-8435

Notes

The authors declare no competing financial interest.

■ ACKNOWLEDGMENTS

We gratefully acknowledge generous support from NanoNed, The Netherlands Organization for Scientific Research (NWO-CW, Top grant to B.L.F. and NWO VIDI grant no. 723.014.001 for W.S.), the Royal Netherlands Academy of Arts and Sciences (KNAW), the Ministry of Education, Culture and Science (Gravitation program 024.001.035), and the European Research Council (Advanced Investigator Grant no. 694345 to B.L.F.).

■ REFERENCES

(1) (a) Brieke, C.; Rohrbach, F.; Gottschalk, A.; Mayer, G.; Heckel, A. Light-Controlled Tools. *Angew. Chem., Int. Ed.* **2012**, *51*, 8446−8476. (b) Feringa, B. L., Browne, W. R. *Molecular Switches*, 2nd ed; Wiley-VCH: Weinheim, 2011. (c) Szymański, W.; Beierle, J. M.; Kistemaker, H. A. V.; Velema, W. A.; Feringa, B. L. Reversible Photocontrol of Biological Systems by the Incorporation of Molecular Photoswitches. *Chem. Rev.* **2013**, *113*, 6114−6178.

(2) (a) Beharry, A. A.; Woolley, G. A. Azobenzene Photoswitches for Biomolecules. *Chem. Soc. Rev.* **2011**, *40*, 4422−4437. (b) Dong, M.; Babalhavaeji, A.; Samanta, S.; Beharry, A. A.; Woolley, G. A. Red-Shifting Azobenzene Photoswitches for in Vivo Use. *Acc. Chem. Res.* **2015**, *48*, 2662−2670. (c) Bléger, D.; Hecht, S. Visible-Light-Activated Molecular Switches. *Angew. Chem., Int. Ed.* **2015**, *54*, 11338−11349.

(3) (a) Irie, M. Diarylethenes for Memories and Switches. *Chem. Rev.* **2000**, *100*, 1685−1716. (b) Okuda, J.; Tanaka, Y.; Kodama, R.; Sumaru, K.; Morishita, K.; Kanamori, T.; Yamazoe, S.; Hyodo, K.; Yamazaki, S.; Miyatake, T.; Yokojima, S.; Nakamura, S.; Uchida, K. Photoinduced Cytotoxicity of a Photochromic Diarylethene *via* Caspase Cascade Activation. *Chem. Commun.* **2015**, *51*, 10957−10960. (c) Chen, X.; Wehle, S.; Kuzmanovic, N.; Merget, B.; Holzgrabe, U.; König, B.; Sotriffer, C. A.; Decker, M. Acetylcholinesterase Inhibitors with Photoswitchable Inhibition of β-Amyloid Aggregation. *ACS Chem. Neurosci.* **2014**, *5*, 377−389.

(4) (a) Willner, I.; Rubin, S.; Cohen, Y. Photoregulated Binding of Spiropyran-Modified Concanavalin A to Monosaccharide-Functionalized Self-Assembled Monolayers on Gold Electrodes. *J. Am. Chem. Soc.* **1993**, *115*, 4937−4938. (b) Velema, W. A.; Hansen, M. J.; Lerch, M. M.; Driessen, A. J.; Szymanski, W.; Feringa, B. L. Ciprofloxacin-Photoswitch Conjugates: A Facile Strategy for Photopharmacology. *Bioconjugate Chem.* **2015**, *26*, 2592−2597. (c) Koçer, A.; Walko, M.; Meijberg, W.; Feringa, B. L. A Light-Actuated Nanovalve Derived from a Channel Protein. *Science* **2005**, *309*, 755−758.

(5) Lachmann, D.; Studte, C.; Männel, B.; Hübner, H.; Gmeiner, P.; König, B. Photochromic Dopamine Receptor Ligands Based on Dithienylethenes and Fulgides. *Chem. - Eur. J.* **2017**, *23*, 13423−13434.

(6) (a) Renner, C.; Moroder, L. Azobenzene as Conformational Switch in Model Peptides. *ChemBioChem* **2006**, *7*, 868−878. (b) Mart, R. J.; Allemann, R. K. Azobenzene Photocontrol of Peptides and Proteins. *Chem. Commun.* **2016**, *52*, 12262−12277. (c) Samanta, S.; Woolley, G. A. Bis-Azobenzene Crosslinkers for Photocontrol of Peptide Structure. *ChemBioChem* **2011**, *12*, 1712−1723. (d) Samanta, S.; Qin, C.; Lough, A. J.; Woolley, G. A. Bidirectional Photocontrol of Peptide Conformation with a Bridged Azobenzene Derivative. *Angew. Chem., Int. Ed.* **2012**, *51*, 6452−6455. (e) Martín-Quirós, A.; Nevola, L.; Eckelt, K.; Madurga, S.; Gorostiza, P.; Giralt, E. Absence of a Stable Secondary Structure is Not a Limitation for Photoswitchable Inhibitors of β-Arrestin/β-Adaptin 2 Protein-Protein Interaction. *Chem. Biol.* **2015**, *22*, 31−37.

(7) (a) Szymański, W.; Yilmaz, D.; Koçer, A.; Feringa, B. L. Bright Ion Channels and Lipid Bilayers. *Acc. Chem. Res.* **2013**, *46*, 2910−2923. (b) Frank, J. A.; Franquelim, H. G.; Schwille, P.; Trauner, D. Optical Control of Lipid Rafts with Photoswitchable Ceramides. *J. Am. Chem. Soc.* **2016**, *138*, 12981−12986.

(8) (a) Blanco, B.; Palasis, K. A.; Adwal, A.; Callen, D. F.; Abell, A. D. Azobenzene-Containing Photoswitchable Proteasome Inhibitors with Selective Activity and Cellular Toxicity. *Bioorg. Med. Chem.* **2017**, *25*, 5050−5054. (b) Hansen, M. J.; Velema, W. A.; de Bruin, G.; Overkleeft, H. S.; Szymanski, W.; Feringa, B. L. Proteasome Inhibitors with Photocontrolled Activity. *ChemBioChem* **2014**, *15*, 2053−2057. (c) Tsai, Y. H.; Essig, S.; James, J. R.; Lang, K.; Chin, J. W. Selective, Rapid and Optically Switchable Regulation of Protein Function in Live Mammalian Cells. *Nat. Chem.* **2015**, *7*, 554−561. (d) Reisinger, B.; Kuzmanovic, N.; Löffler, P.; Merkl, R.; König, B.; Sterner, R. Exploiting Protein Symmetry to Design Light-Controllable Enzyme Inhibitors. *Angew. Chem., Int. Ed.* **2014**, *53*, 595−598.

(9) (a) Lubbe, A. S.; Szymanski, W.; Feringa, B. L. Recent Developments in Reversible Photoregulation of Oligonucleotide Structure and Function. *Chem. Soc. Rev.* **2017**, *46*, 1052−1079. (b) Wang, F.; Liu, X.; Willner, I. DNA Switches: from Principles to Applications. *Angew. Chem., Int. Ed.* **2015**, *54*, 1098−1129. (c) Nakasone, Y.; Ooi, H.; Kamiya, Y.; Asanuma, H.; Terazima, M. Dynamics of Inter-DNA Chain Interaction of Photoresponsive DNA. *J. Am. Chem. Soc.* **2016**, *138*, 9001−9004. (d) Ogasawara, S.; Maeda, M. Straightforward and Reversible Photoregulation of Hybridization by Using a Photochromic Nucleoside. *Angew. Chem., Int. Ed.* **2008**, *47*, 8839−8842. (e) Wang, H. X.; Xi, D. D.; Xie, M. S.; Wang, H. X.; Qu, G. R.; Guo, H. M. Nucleoside-Based Diarylethene Photoswitches: Synthesis and Photochromic Properties. *ChemBioChem* **2016**, *17*, 1216−1220. (f) Lubbe, A. S.; Liu, Q.; Smith, S. J.; de Vries, J. W.; Kistemaker, J. C. M.; de Vries, A. H.; Faustino, I.; Meng, Z.; Szymanski, W.; Herrmann, A.; Feringa, B. L. Photoswitching of DNA Hybridization Using a Molecular Motor. *J. Am. Chem. Soc.* **2018**, *140*, 5069−5076.

(10) (a) Lerch, M. M.; Hansen, M. J.; van Dam, G. M.; Szymanski, W.; Feringa, B. L. Emerging Targets in Photopharmacology. *Angew. Chem., Int. Ed.* **2016**, *55*, 10978−10999. (b) Broichhagen, J.; Frank, J. A.; Trauner, D. A Roadmap to Success in Photopharmacology. *Acc. Chem. Res.* **2015**, *48*, 1947−1960. (c) Velema, W. A.; Szymanski, W.; Feringa, B. L. Photopharmacology: Beyond Proof of Principle. *J. Am. Chem. Soc.* **2014**, *136*, 2178−2191.

(11) (a) Velema, W. A.; van der Berg, J. P.; Hansen, M. J.; Szymanski, W.; Driessen, A. J.; Feringa, B. L. Optical Control of Antibacterial Activity. *Nat. Chem.* **2013**, *5*, 924−928. (b) Wegener, M.; Hansen, M. J.; Driessen, A. J. M.; Szymanski, W.; Feringa, B. L. Photocontrol of Antibacterial Activity: Shifting from UV to Red Light Activation. *J. Am. Chem. Soc.* **2017**, *139*, 17979−17986. (c) Babii, O.; Afonin, S.; Berditsch, M.; Reiβer, S.; Mykhailiuk, P. K.; Kubyshkin, V. S.; Steinbrecher, T.; Ulrich, A. S.; Komarov, I. V. Controlling Biological Activity with Light: Diarylethene-Containing Cyclic Peptidomimetics. *Angew. Chem., Int. Ed.* **2014**, *53*, 3392−3395.

(12) (a) Tochitsky, I.; Polosukhina, A.; Degtyar, V. E.; Gallerani, N.; Smith, C. M.; Friedman, A.; Van Gelder, R. N.; Trauner, D.; Kaufer, D.; Kramer, R. H. Restoring Visual Function to Blind Mice with a Photoswitch that Exploits Electrophysiological Remodeling of Retinal Ganglion Cells. *Neuron* **2014**, *81*, 800−813. (b) Polosukhina, A.; Litt, J.; Tochitsky, I.; Nemargut, J.; Sychev, Y.; De Kouchkovsky, I.; Huang, T.; Borges, K.; Trauner, D.; Van Gelder, R. N.; Kramer, R. H. Photochemical Restoration of Visual Responses in Blind Mice. *Neuron* **2012**, *75*, 271−282.

(13) (a) Stein, M.; Middendorp, S. J.; Carta, V.; Pejo, E.; Raines, D. E.; Forman, S. A.; Sigel, E.; Trauner, D. Azo-Propofols: Photochromic Potentiators of $GABA_A$Receptors. *Angew. Chem., Int. Ed.* **2012**, *51*, 10500−10504. (b) Pittolo, S.; Gómez-Santacana, X.; Eckelt, K.; Rovira, X.; Dalton, J.; Goudet, C.; Pin, J. P.; Llobet, A.; Giraldo, J.; Llebaria, A.; Gorostiza, P. An Allosteric Modulator to Control Endogenous G Protein-Coupled Receptors with Light. *Nat. Chem. Biol.* **2014**, *10*, 813−815.

(14) (a) Borowiak, M.; Nahaboo, W.; Reynders, M.; Nekolla, K.; Jalinot, P.; Hasserodt, J.; Rehberg, M.; Delattre, M.; Zahler, S.; Vollmar, A.; Trauner, D.; Thorn-Seshold, O. Photoswitchable Inhibitors of Microtubule Dynamics Optically Control Mitosis and Cell Death. *Cell* **2015**, *162*, 403−411. (b) Engdahl, A. J.; Torres, E. A.; Lock, S. E.; Engdahl, T. B.; Mertz, P. S.; Streu, C. N. Synthesis, Characterization, and Bioactivity of the Photoisomerizable Tubulin Polymerization Inhibitor Azo-Combretastatin A4. *Org. Lett.* **2015**, *17*, 4546−4549. (c) Sheldon, J. E.; Dcona, M. M.; Lyons, C. E.; Hackett, J. C.; Hartman, M. C. Photoswitchable Aanticancer Aactivity *via Trans*−*Cis* Isomerization of a Combretastatin A4 analog. *Org. Biomol. Chem.* **2016**, *14*, 40−49.

(15) Szymanski, W.; Ourailidou, M. E.; Velema, W. A.; Dekker, F. J.; Feringa, B. L. Light-Controlled Histone Deacetylase (HDAC) Inhibitors: Towards Photopharmacological Chemotherapy. *Chem. - Eur. J.* **2015**, *21*, 16517−16524.

(16) Ferreira, R.; Nilsson, J. R.; Solano, C.; Andréasson, J.; Grøtli, M. Design, Synthesis and Inhibitory Activity of Photoswitchable RET Kinase Inhibitors. *Sci. Rep.* **2015**, *5*, 9769.

(17) (a) Broichhagen, J.; Frank, J. A.; Johnston, N. R.; Mitchell, R. K.; Šmid, K.; Marchetti, P.; Bugliani, M.; Rutter, G. A.; Trauner, D.; Hodson, D. J. A Red-Shifted Photochromic Sulfonylurea for the Remote Control of Pancreatic Beta Cell Function. *Chem. Commun.* **2015**, *51*, 6018−6021. (b) Broichhagen, J.; Schönberger, M.; Cork, S. C.; Frank, J. A.; Marchetti, P.; Bugliani, M.; Shapiro, A. M.; Trapp, S.; Rutter, G. A.; Hodson, D. J.; Trauner, D. Optical Control of Insulin Release Using a Photoswitchable Sulfonylurea. *Nat. Commun.* **2014**, *5*, 5116.

(18) Koumura, N.; Zijlstra, R. W.; van Delden, R. A.; Harada, N.; Feringa, B. L. Light-Driven Monodirectional Molecular Rotor. *Nature* **1999**, *401*, 152−155.

(19) (a) Kassem, S.; van Leeuwen, T.; Lubbe, A. S.; Wilson, M. R.; Feringa, B. L.; Leigh, D. A. Artificial Molecular Motors. *Chem. Soc. Rev.* **2017**, *46*, 2592−2621. (b) Erbas-Cakmak, S.; Leigh, D. A.; McTernan, C. T.; Nussbaumer, A. L. Artificial Molecular Machines. *Chem. Rev.* **2015**, *115*, 10081−10206. (c) Pezzato, C.; Cheng, C.; Stoddart, J. F.; Astumian, R. D. Mastering the Non-Equilibrium Assembly and Operation of Molecular Machines. *Chem. Soc. Rev.* **2017**, *46*, 5491−5507. (d) Kelly, T. R.; De Silva, H.; Silva, R. A. Unidirectional Rotary Motion in a Molecular System. *Nature* **1999**, *401*, 150−152. (e) Kelly, T. R.; Bowyer, M. C.; Bhaskar, K. V.; Bebbington, D.; Garcia, A.; Lang, F.; Kim, M. H.; Jette, M. P. A Molecular Brake. *J. Am. Chem. Soc.* **1994**, *116*, 3657−3658. (f) Jimenez, M. C.; Dietrich-Buchecker, C.; Sauvage, J.-P. Towards Synthetic Molecular Muscles: Contraction and Stretching of a Linear Rotaxane Dimer. *Angew. Chem., Int. Ed.* **2000**, *39*, 3284−3287. (g) Muraoka, T.; Kinbara, K.; Aida, T. Mechanical Twisting of a Guest by a Photoresponsive Host. *Nature* **2006**, *440*, 512−515. (h) van Leeuwen, T.; Lubbe, A. S.; Štacko, P.; Wezenberg, S. J.; Feringa, B. L. Dynamic Control of Function by Light-Driven Molecular Motors. *Nat. Rev. Chem.* **2017**, *1*, 96. (i) Roke, D.; Wezenberg, S. J.; Feringa, B. L. Molecular Rotary Motors: Unidirectional Motion around Double Bonds. *Proc. Natl. Acad. Sci. U. S. A.* **2018**, 201712784.

(20) Koumura, N.; Geertsema, E. M.; Van Gelder, M. B.; Meetsma, A.; Feringa, B. L. Second Generation Light-Driven Molecular Motors. Unidirectional Rotation Controlled by a Single Stereogenic Center with Near-Perfect Photoequilibria and Acceleration of the Speed of Rotation by Structural Modification. *J. Am. Chem. Soc.* **2002**, *124*, 5037−5051.

(21) Vicario, J.; Walko, M.; Meetsma, A.; Feringa, B. L. Fine Tuning of the Rotary Motion by Structural Modification in Light-Driven Unidirectional Molecular Motors. *J. Am. Chem. Soc.* **2006**, *128*, 5127−5135.

(22) Klok, M.; Walko, M.; Geertsema, E. M.; Ruangsupapichat, N.; Kistemaker, J. C. M.; Meetsma, A.; Feringa, B. L. New Mechanistic Insight in the Thermal Helix Inversion of Second-Generation Molecular Motors. *Chem. - Eur. J.* **2008**, *14*, 11183−11193.

DOI: 10.1021/acs.joc.8b01627
J. Org. Chem. 2018, 83, 11008−11018

(23) Wang, J.; Feringa, B. L. Dynamic Control of Chiral Space in a Catalytic Asymmetric Reaction Using a Molecular Motor. *Science* **2011**, *331*, 1429−1432.
(24) Eelkema, R.; Pollard, M. M.; Vicario, J.; Katsonis, N.; Ramon, B. S.; Bastiaansen, C. W. M.; Broer, D. J.; Feringa, B. L. Molecular Machines: Nanomotor Rotates Microscale Objects. *Nature* **2006**, *440*, 163.
(25) Vlatkovic, M.; Feringa, B. L.; Wezenberg, S. J. Dynamic Inversion of Stereoselective Phosphate Binding to a Bisurea Receptor Controlled by Light and Heat. *Angew. Chem., Int. Ed.* **2016**, *55*, 1001−1004.
(26) Wezenberg, S. J.; Croisetu, C. M.; Stuart, M. C. A.; Feringa, B. L. Reversible Gel−Sol Photoswitching with an Overcrowded Alkene-Based Bis-Urea Supergelator. *Chem. Sci.* **2016**, *7*, 4341−4346.
(27) Van Dijken, D. J.; Chen, J.; Stuart, M. C. A.; Hou, L.; Feringa, B. L. Amphiphilic Molecular Motors for Responsive Aggregation in Water. *J. Am. Chem. Soc.* **2016**, *138*, 660−669.
(28) Poloni, C.; Stuart, M. C. A.; van der Meulen, P.; Szymanski, W.; Feringa, B. L. Light and Heat Control over Secondary Structure and Amyloid-like Fiber Formation in an Overcrowded-Alkene-Modified Trp Zipper. *Chem. Sci.* **2015**, *6*, 7311−7318.
(29) van Delden, R. A.; ter Wiel, M. K. J.; Pollard, M. M.; Vicario, J.; Koumura, N.; Feringa, B. L. Unidirectional Molecular Motor on a Gold Surface. *Nature* **2005**, *437*, 1337−1340.
(30) London, G.; Carroll, G. T.; Fernández Landaluce, T.; Pollard, M. M.; Rudolf, P.; Feringa, B. L. Light-Driven Altitudinal Molecular Motors on Surfaces. *Chem. Commun.* **2009**, 1712−1714.
(31) Chen, K.-Y.; Ivashenko, O.; Carroll, G. T.; Robertus, J.; Kistemaker, J. C. M.; London, G. G.; Browne, W. R.; Rudolf, P.; Feringa, B. L. Control of Surface Wettability Using Tripodal Light-Activated Molecular Motors. *J. Am. Chem. Soc.* **2014**, *136*, 3219−3224.
(32) Kudernac, T.; Ruangsupapichat, N.; Parschau, M.; Maciá, B.; Katsonis, N.; Harutyunyan, S. R.; Ernst, K.-H.; Feringa, B. L. Electrically Driven Directional Motion of a Four-Wheeled Molecule on a Metal Surface. *Nature* **2011**, *479*, 208−211.
(33) Kistemaker, J. C. M.; Štacko, P.; Visser, J.; Feringa, B. L. Unidirectional Rotary Motion in Achiral Molecular Motors. *Nat. Chem.* **2015**, *7*, 890−896.
(34) Nagatsugi, F.; Takahashi, Y.; Kobayashi, M.; Kuwahara, S.; Kusano, S.; Chikuni, T.; Hagihara, S.; Harada, N. Synthesis of Peptide-Conjugated Light-Driven Molecular Motors and Evaluation of their DNA-Binding Properties. *Mol. BioSyst.* **2013**, *9*, 969−973.
(35) Wezenberg, S. J.; Vlatkovic, M.; Kistemaker, J. C. M.; Feringa, B. L. Multi-State Regulation of the Dihydrogen Phosphate Binding Affinity to a Light- and Heat-Responsive Bis-Urea Receptor. *J. Am. Chem. Soc.* **2014**, *136*, 16784−16787.
(36) García-López, V.; Chen, F.; Nilewski, L. G.; Duret, G.; Aliyan, A.; Kolomeisky, A. B.; Robinson, J. T.; Wang, G.; Pal, R.; Tour, J. M. Molecular Machines Open Cell Membranes. *Nature* **2017**, *548*, 567−572.
(37) Van Leeuwen, T.; Gan, J.; Kistemaker, J. C. M.; Pizzolato, S. F.; Chang, M. C.; Feringa, B. L. Enantiopure Functional Molecular Motors Obtained by a Switchable Chiral-Resolution Process. *Chem. - Eur. J.* **2016**, *22*, 7054−7058.
(38) Ter Wiel, M. K. J.; Van Delden, R. A.; Meetsma, A.; Feringa, B. L. Light-Driven Molecular Motors: Stepwise Thermal Helix Inversion during Unidirectional Rotation of Sterically Overcrowded Biphenanthrylidenes. *J. Am. Chem. Soc.* **2005**, *127*, 14208−14222.
(39) Pollard, M. M.; Meetsma, A.; Feringa, B. L. A Redesign of Light-Driven Rotary Molecular Motors. *Org. Biomol. Chem.* **2008**, *6*, 507−512.
(40) Greenspan, P.; Fowler, S. D. Spectrofluorometric Studies of the Lipid Probe, Nile Red. *J. Lipid Res.* **1985**, *26*, 781−789.
(41) Nekipelova, T. D.; Shishkov, V. S.; Kuzmin, V. A. Mechanism of Photoinduced Addition of Water and Methanol to the Double Bond of 1,2-Dihydroquinolines. *High Energy Chem.* **2002**, *36*, 183−188.
(42) Koumura, N.; Geertsema, E. M.; Meetsma, A.; Feringa, B. L. Light-Driven Molecular Rotor: Unidirectional Rotation Controlled by a Single Stereogenic Center. *J. Am. Chem. Soc.* **2000**, *122*, 12005−12006.
(43) Pollard, M. M.; Klok, M.; Pijper, D.; Feringa, B. L. Rate Acceleration of Light-Driven Rotary Molecular Motors. *Adv. Funct. Mater.* **2007**, *17*, 718−729.
(44) Vicario, J.; Meetsma, A.; Feringa, B. L. Controlling the Speed of Rotation in Molecular Motors. Dramatic Acceleration of the Rotary Motion by Structural Modification. *Chem. Commun.* **2005**, 5910−5912.
(45) Kulago, A. Nanotechnological Tools Built on Synthetic Light-Driven Molecular Motors. PhD thesis, University of Groningen.
(46) Pijper, D.; Feringa, B. L. Molecular Transmission: Controlling the Twist Sense of a Helical Polymer with a Single Light-Driven Molecular Motor. *Angew. Chem., Int. Ed.* **2007**, *46*, 3693−3696.
(47) Gottlieb, H. E.; Kotlyar, V.; Nudelman, A. NMR Chemical Shifts of Common Laboratory Solvents as Trace Impurities. *J. Org. Chem.* **1997**, *62*, 7512−7515.

DOI: 10.1021/acs.joc.8b01627
J. Org. Chem. 2018, 83, 11008−11018